Demonstration of Ripple Reduction by Ferritic Steel Board Insertion in JFT-2M

H.KAWASHIMA 1), M.SATO 1), K.TSUZUKI 1), Y.MIURA 1), N.ISEI 1), H.KIMURA 1), T.NAKAYAMA 2), M.ABE 2), D.S.DARROW 3), and JFT-2M GROUP 1)

1) Japan Atomic Energy Research Institute, Tokai, Naka, Ibaraki Japan
2) Hitachi Ltd., Hitachi, Ibaraki Japan
3) Princeton Plasma Physics Laboratory, Princeton, New Jersey U.S.A

e-mail contact of main author: kawasimh@fusion.naka.jaeri.go.jp

Abstract. In the JFT-2M tokamak, application testing of low activation ferritic steel to plasma has been investigated, (so called Advanced Material Tokamak Experiment (AMTEX) program). In the first stage, toroidal field ripple reduction was examined by ferritic steel boards (FBs) insertion between toroidal field coils and vacuum vessel. It is demonstrated that the FB insertion is effective to reduce the toroidal field ripple and to reduce the losses of fast ions produced by tangential co-NBI. By optimizing the FB thickness, such that the fundamental mode ripple is minimized to be 0.07% at the shoulder part, the ripple-trapped loss is reduced to be almost negligible. It is indicated that the reductions of the fundamental mode ripple and the ripple banana diffusion coefficient at the shoulder part are most effective to reduce the ripple ion losses. Ripple loss reduction by FBs is also confirmed with the perpendicular beam injection. The FB insertion gives no deteriorative effect on the plasma production and control.

1. Introduction

The reduced-activation ferritic steel 'F82H' is one of the promising candidate materials for fusion reactors from the properties of relatively low activation, low swelling and high heat-resistance [1,2]. However, ferromagnetic material such as ferritic steel has not been used in fusion devices until very recently because it was worried about to disturb the magnetic fields. The effect of ferritic steel to tokamak plasma was first investigated experimentally in a small tokamak HT2 with installing ferritic steel inside the vacuum vessel. It was shown that the normal discharges were possible [3,4]. However, the effect on the plasma stability and compatibility with improved confinement has not been made clear yet. Another benefit to use the ferritic steel, if compatible with plasma, is to reduce the toroidal field ripple and to reduce ripple losses [5-8]. In tokamak devices, a small amount of toroidal field ripple (a few percent) enlarges the radial diffusion loss of fast ions. It is recognized that fast ion loss due to the ripple causes thermal damage on the first wall and this is one of the critical points for the ITER steady state operation scenario [9]. In order to solve this problem, the design of ripple reduction by using ferromagnetic material is going on for ITER.

In the JFT-2M tokamak ($R=1.31$m, $a\leq 0.35$m, $\kappa\leq 1.7$, $B_{t0}\leq 2.2$T), Advanced Material Tokamak Experiment (AMTEX) is being in progress for the demonstration of compatibility of the ferritic steel with high performance plasma [8,10-17]. AMTEX consists of three stages. In the first stage, the toroidal field ripple reduction has been investigated with ferritic steel boards (FBs) outside the vacuum vessel. For the investigation of both magnetic effects and plasma-surface interaction with ferritic steel, FBs are installed inside the JFT-2M vacuum vessel in the second stage (partial (20%) covering of the inside wall) and the third stage (full covering) [17].

In this paper, we describe the results in the first stage. Section 2 gives the outline of FB insertion. Section 3 shows that the fast ion loss due to the ripple is made sure before FB insertion by infrared TV. Section 4 describes that the surface temperature increment of first

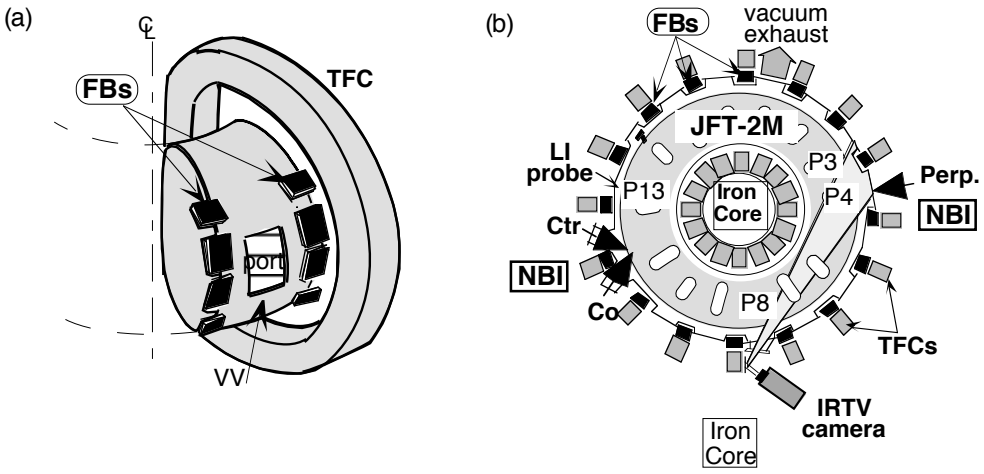

Fig.1 (a): Illustration of ferritic steel board (FB) insertion on JFT-2M. FBs are installed between the vacuum vessel and TFCs in all (16) toroidal sections. (b): Toroidal arrangements of FBs, neutral beam injectors, and IRTV and LI probe for fast loss ion diagnostics.

wall due to the ripple-trapped or banana drift losses are reduced successfully by FB insertion during tangential beam injection. In section 5, reduction of fast ion losses during perpendicular beam injection is described. The other effects of ferromagnetic FBs to plasma are presented in section 6. Summary is given in section 7.

2. Ferritic Steel Board Insertion on JFT-2M

Figure 1 shows the schematic view of FB insertion to demonstrate the effect of ripple reduction. FBs have been installed between the vacuum vessel (VV) and toroidal field coils (TFCs) in all (16) toroidal sections [11-16]. Basically 4 blocks of FBs cover discretely the poloidal angle ±65° in the outboard side from the upper and lower shoulder parts to the equatorial plane part. Inserting FBs just under TFCs, toroidal magnetic field around under TFCs is weakened and that between TFCs is strengthened since magnetic flux comes out from the ferritic steel. As a result, the fundamental mode ripple (δ_{16}) is reduced in principle as shown in Fig.2. But, there is a possibility that the second harmonic mode ripple (δ_{32}) or more higher mode ripple grows up with complicated magnetic structure with FBs [8,10,11] and enlarges significantly the ripple banana diffusion coefficient [18], assuming that it is proportional to the $\Sigma_{16,32} n^{2.25} \delta_n^{1.5}$ with higher mode ripple. Here n is toroidal mode number and δ_n is ripple amplitude.

Therefore, thickness, width and position of FBs were determined to reduce both δ_{16} and δ_{32} and to minimize $\Sigma_{16,32} n^{2.25} \delta_n^{1.5}$ under restriction that FBs must be installed to avoid the existing facilities (coils, heating system, or any diagnostics) [11,12]. In experiments, FBs of 50mm (FB1) and 67mm (FB2) in thickness were employed. Figure 3 indicates δ_{16} and δ_{32} of the two cases at the equatorial plane part and the shoulder part

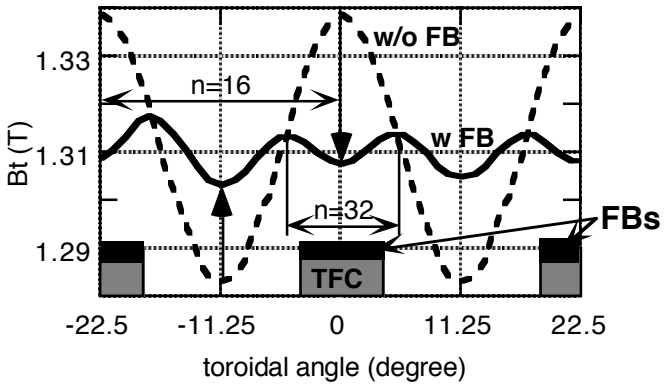

Fig.2 Toroidal field profiles without and with FBs at outer edge of plasma (R=1.6m, Z=0.0m). This is an example when 67mm thickness FBs(FB2) are set in JFT-2M at B_{t0}=1.6T on 2/16 sections.

for toroidal field B_{t0}=1.0T~2.2T. Since F82H has a specific permeability μ_s=2~3.5 for B_{t0}=1.0T~2.2T with saturated magnetization M_s=1.96T [2], the ripple amplitude changes widely by changing thickness of FBs and B_{t0} [10,11]. Note that both fundamental and second harmonic mode ripple at the shoulder part ($\delta_{16}{}^s$ and $\delta_{32}{}^s$) can be almost zero with FB2 at B_{t0}=1.0T and $\Sigma_{16,32}n^{2.25}(\delta_n{}^s)^{1.5}$ is minimized, although those at the equatorial plane part becomes large. Fast ion losses due to the ripple have been investigated on these wide parameter regions.

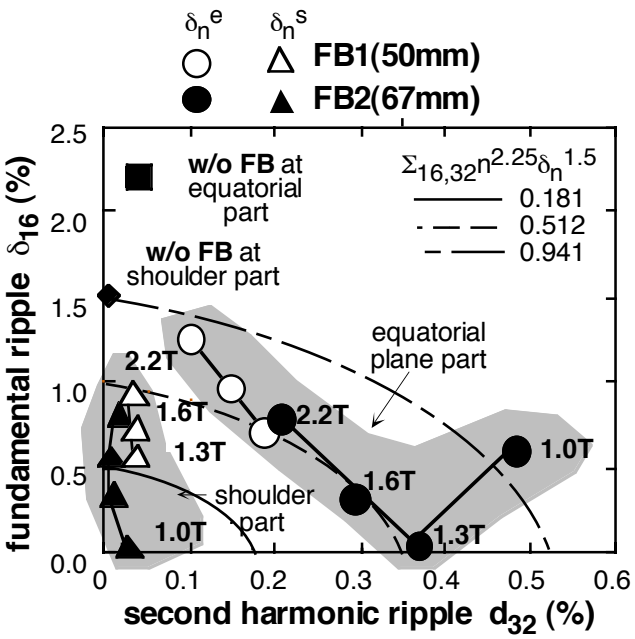

Fig.3 Relations between fundamental ripple (δ_{16}) and second harmonic ripple (δ_{32}) at the shoulder part (R=1.5m,Z=±0.25m) and equatorial plane part (R=1.6m,Z=0.0m) without FB, with FB1and with FB2 at B_{t0}=1.0T~2.2T, respectively. Contour lines of $\Sigma_{16,32}n^{2.25}\delta_n{}^{1.5}$ are also indicated.

3. Observation of Fat Ion Loss due to the Ripple

The fast ion losses due to the toroidal field ripple are caused by the ripple well trapping (ripple-trapped: RT loss) and banana drift diffusion (banana drift: BD loss). To evaluate the fast ion losses, infrared TV camera (IRTV) and lost ion (LI) probe were installed as shown in Fig.1 (b). IRTV measures the first wall temperature increment due to the ripple loss [19]. The viewing area is in the outboard wall around P3 and P4 ports as indicated Fig.1 (b), which is covered by the carbon tiles with a good emissivity. In order to detect the losses due to the banana drift at D-shaped plasma configuration, we set the carbon tiles at the nearest position to the last closed surface of plasma on the equatorial plane part. Major radius of the tile surface is 1.628m where is 0.097m away from the vacuum vessel wall. The plasma is limited by the tiles. The LI probe measures gyroradius (i.e. energy) and pitch angle of the lost fast ion [20]. The probe head is located on P13 upper shoulder part around the ripple-trapped loss regions. The fast ions are produced by 36keV hydrogen beam injection from tangential and perpendicular directions. Tangential NBI (co and counter) are injected from P11 and P12, respectively, at injection angle (θ_{in}) of 38°. Perpendicular NBI is injected from P4 at θ_{in} =80°.

The experiments were performed with B_{t0}=1.0T~2.2T, plasma current I_p=150kA~250kA (direction of I_p is clockwise), line averaged density $\overline{n_e}$=1~3x$10^{19}m^{-3}$, and limiter D-shaped configuration. Figure 4(a) shows the expectation of RT and BD loss regions from the ripple well on the poloidal cross section. Figure 4 (b) shows also geometrical position of hot spots by them on the first wall in IRTV viewing sight. When the ion grad B drift direction is downward (B_t direction is clockwise (CW)), the RT loss regions are expected to locate on the shoulder part (i.e. #2 carbon tiles in the figure) between adjacent TFCs. The BD loss regions locate around outer equatorial plane in P3 side on the D-shaped plasmas because the first wall on #6~#7 carbon tiles is nearest to the plasma as mentioned above and the field line comes from the left on Fig.4 (b). Figure 4(c) shows that an infrared image during the tangential co-NBI (~500kW) before FB insertion at B_{t0}=1.3T and Ip=200kA. Hot spots due to RT loss are

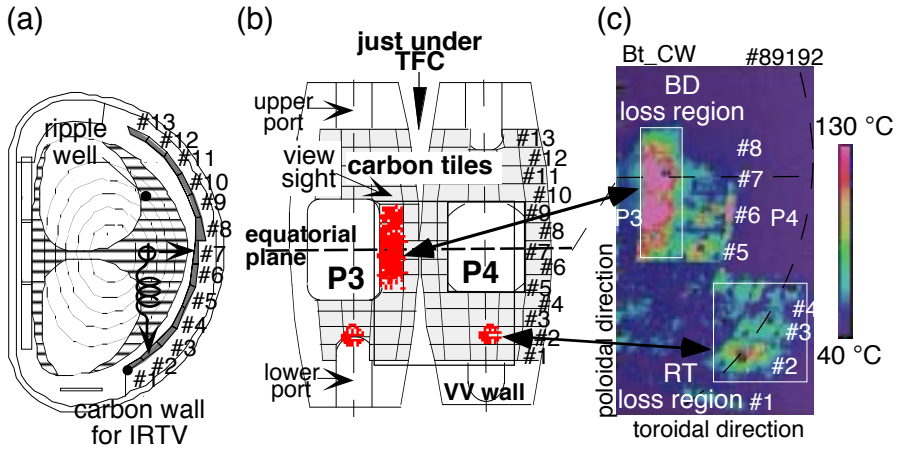

Fig.4 (a) Expectation of RT and BD loss regions from ripple well at the D-shaped plasma on experiment for B_{t0}=1.3T, I_p=200kA. (b) Geometrical position of hot spots on the first wall in P3-P4 of IRTV viewing sight. (c) Infrared image by IRTV during tangential co-NBI (36keV, ~500kW) before FB insertion.

observed clearly at shoulder part just under P4 port and that of BD loss at equatorial plane near the P3 port side between P3 and P4 of the BD loss regions. These locations agree well with the expectation. The maximum temperature on the RT and BD loss regions reach to ~120°C and ~190°C, respectively, in that case. Since the temperature increment under P4 disappeared when the ion grad B direction was reversed (Bt direction was counter clockwise (CCW)), it was confirmed that the hot spot at the shoulder part is due to RT loss.

Figure 5 shows a result of LI probe measurement during co-NBI after FB insertion. The loss ions which pitch angle corresponds to loss cone on the velocity space detected on left side on the figure. Ripple-trapped loss ions are also detected at a pitch angle close to 90° on right side. We can obtain a clear view that the fast ions are slowing down and lost around 25keV.

4. Reduction of Fast Ion Loss by Ferritic Steel Board during co-NBI

We describe here the experimental results that the surface temperature increment (ΔT_s) due to RT and BD losses are reduced successfully by FB insertion. Figures 6(a) and (b) shows ΔT_s profiles at BD and RT loss regions in the cases without FB, with FB1 (50mm) and with FB2 (67mm), respectively. Safety factor q_s ,which is a function of the ripple well parameter [21], holds on around 6 to investigate the relations between ΔT_s and the ripple amplitude apart from q_s dependence.

After FB1 insertion, the hot spot due to RT loss under the horizontal port shifts around 6cm outward in the major radius direction (upward in the figure) and the highest temperature increment ($\Delta T_{s\text{-}max}$) decreases from ~75°C to ~50°C. The $\Delta T_{s\text{-}max}$ on the BD loss region around the equatorial plane are also decreased from ~150°C to ~100°C. When FB thickness was increased from 50mm to 67mm, temperature increment almost disappears on RT loss region at B_{t0}=1.0T (shoulder part ripple δ_{16}^{s}=0.068%) as shown in Fig. 6. The $\Delta T_{s\text{-}max}$ by BD loss became also smallest (~70°C) with a broadened

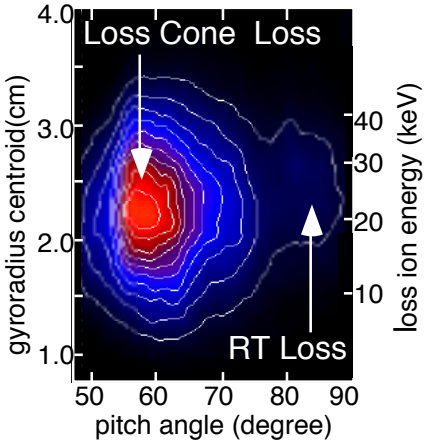

Fig.5 LI probe data during tangential co-NBI when the ion grad B direction is toward the probe.

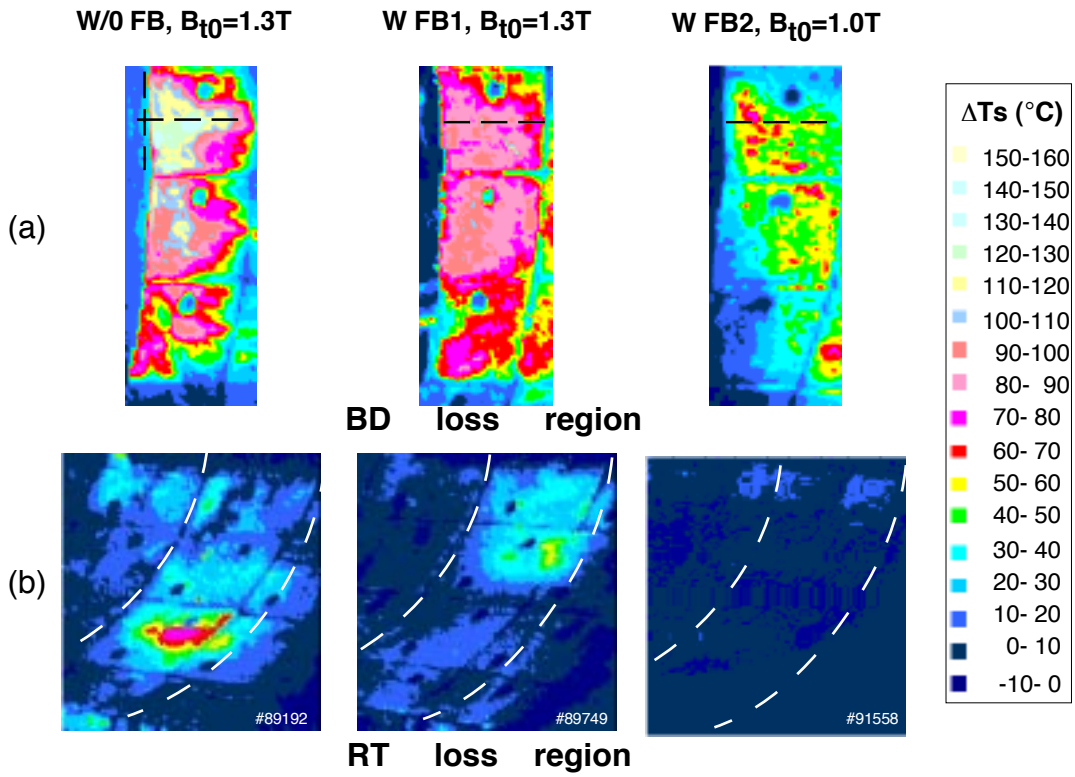

Fig. 6 Surface temperature increment (ΔT_s) on (a) BD and (b)RT loss regions in the cases without FB (B_{t0} =1.3T), with FB1 (B_{t0} =1.3T) and with FB2 (B_{t0} =1.0T) at q_s~6.

profile. These RT loss behaviors correspond to the ripple reduction and the outward shift of ripple well boundary consistently.

From the point of ripple amplitude and ripple banana diffusion coefficient, the change of temperature increment on both RT and BD losses is discussed here. Figure 7 shows the dependence of $\Delta T_{s\text{-}max}$ on the ripple amplitude and the value of $\Sigma_{16,32} n^{2.25} \delta_n^{1.5}$, which is related to the ripple banana diffusion coefficient. Here the ripple amplitude is used the summation of δ_{16} and δ_{32} at the shoulder part ($\Sigma_{16,32}\delta_n^{s}$) and averaged them between the shoulder and equatorial plane parts ($\Sigma_{16,32}\langle\delta_n\rangle$), respectively. The $\Delta T_{s\text{-}max}$ on RT loss region is plotted in Fig.7 (a-1), (a-2) as a function of that ripple amplitude because the ripple well is formed depending on the ripple amplitude. These plots indicate that $\Delta T_{s\text{-}max}$ is reduced according to the shoulder part ripple rather than the averaged ripple. Furthermore, it depends strongly on δ_{16}^{s} because δ_{16}^{s} is much larger than δ_{32}^{s} as seen in Fig.3. For BD loss region, $\Delta T_{s\text{-}max}$ is plotted in Fig.7 (b-1), (b-2) as a function of $\Sigma_{16,32} n^{2.25} \delta_n^{1.5}$. The temperature increment also decreases with decrease of $\Sigma_{16,32} n^{2.25} (\delta_n^{s})^{1.5}$ rather than $\Sigma_{16,32} n^{2.25} \langle\delta_n\rangle^{1.5}$. The reason that the temperature increment is kept at ~70°C even $\Sigma_{16,32} n^{2.25} (\delta_n^{s})^{1.5}$~0 may be caused by orbit losses independent of the ripple amplitude. Thus, these results indicate that both RT and BD losses depend strongly on the ripple amplitude of shoulder part. On the other hand, the effect of δ_{32} at the experiments is not clear enough yet because δ_{32} is very small at the shoulder part. But, the effect of δ_{32} seems to appear on the equatorial part where a broadened profile for the BD loss is made at low B_t with FB2 as indicated in Fig.6(a), because δ_{32} is much larger at the equatorial plane and also the fundamental mode ripple becomes reversal.

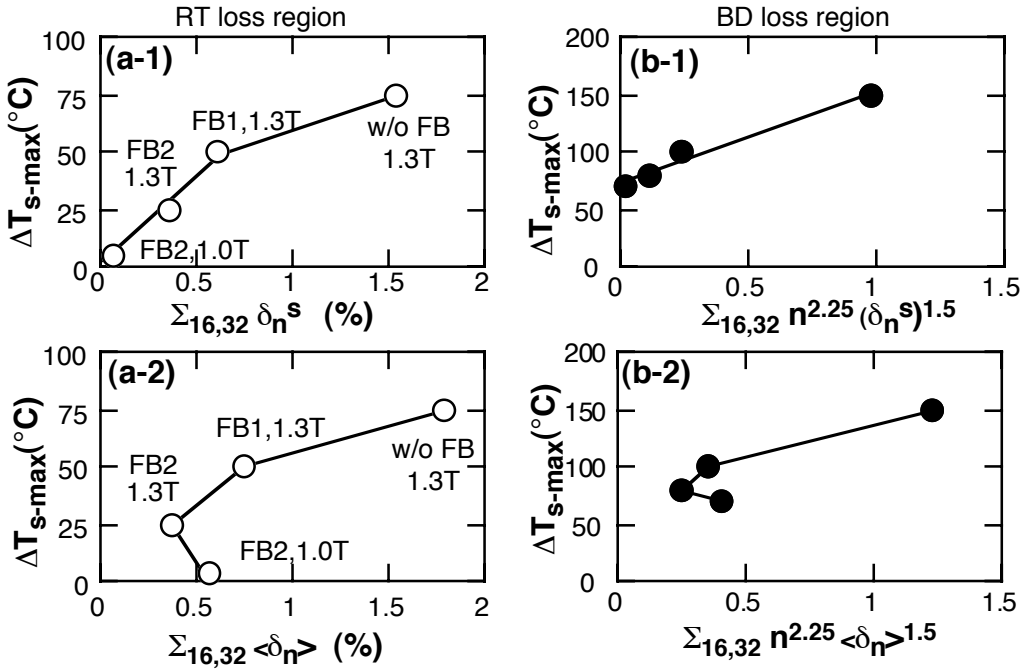

Fig.7 Dependences of $\Delta T_{s\text{-}max}$ on ripple amplitude for RT loss region and the value related the diffusion coefficient for BD loss region without FB, with FB1 and with FB2. B_{t0}=1.0T and 1.3T.

5. Effect of FB during Perpendicular Beam Injection

Fast ion loss due to the ripple was compared between tangential co-NBI and perpendicular NBI. In case of tangential co-injection, a part of the scattered fast ions on outside describe the banana orbit. The banana orbit ions at the turning point have no parallel velocity component ($v_{//}$) and are trapped in the ripple well statistically. For quasi-perpendicular injection, the $v_{//}$ component of the most ions is small originally and they are trapped in the ripple well easily. Relatively large power loss fraction may be produced in this case. Figure 8 shows the comparison for $\Delta T_{s\text{-}max}/P_{in}$ on RT and BD loss regions between co-NBI and perpendicular NBI as a function of the ripple amplitude and the value related to the diffusion coefficient. The injection power is around 500kW for co-NBI and around 40kW for perpendicular NBI. The $\Delta T_{s\text{-}max}/P_{in}$ on RT loss region is about eight times larger than that by co-NBI at the amplitude of 0.6%. Those for RT and BD loss regions at the perpendicular NBI are decreased with decrease of $\Sigma_{16,32}\delta_n^s$ and

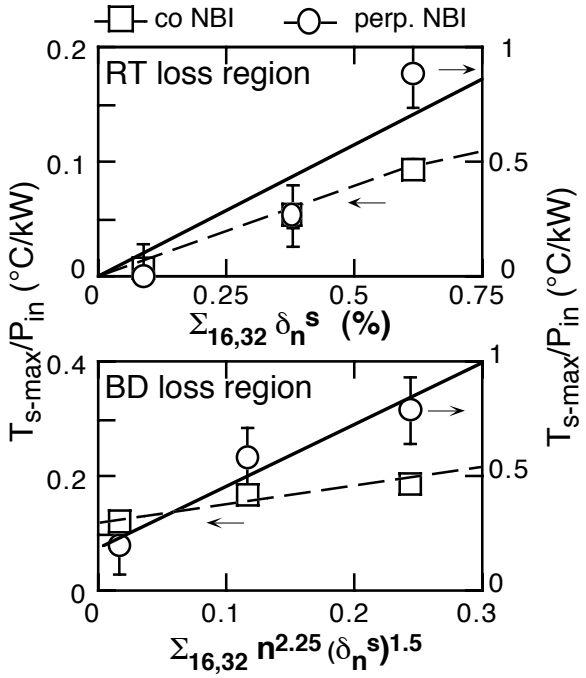

Fig.8 $\Delta T_{s\text{-}max}/P_{in}$ vs $\Sigma_{16,32}\delta_n^s$ and $\Sigma_{16,32}n^{2.25}(\delta_n^s)^{1.5}$ on RT and BD loss regions during co-NBI (P_{in}~ 500kW) and perpendicular NBI (P_{in} ~ 40kW), respectively.

$\Sigma_{16,32} n^{2.25} (\delta_n^S)^{1.5}$ similar as in the case of co-NBI. Thus, the reduction of fast ion loss by FBs during perpendicular beam injection is also confirmed.

6. Effect of Ferromagnetic FBs to Plasmas

No deteriorative effect of FB insertion on the plasma production and control has been observed so far [12,13]. The confinement at L-mode follows the ITER89P L-mode scaling as before [13]. H-mode at single null divertor configurations was obtained easily and the toroidal rotation velocity just inside of separatrix with co-NBI increases from 20-30km/s to 50-60km/s after FB insertion [16]. This is favorable to avoid an occurrence of locked mode by the error fields [22].

An error field of m=2, n=1 mode was enhanced artificially to $B_{r\ (m/n=2/1)} / B_t \sim 1 \times 10^{-4}$ by taking off 40% FB (FB2) continuously in the toroidal direction. This error field corresponds to ~40% of the critical field to lead to the locked mode disruption. But even in this condition, the regions of locked mode disruption and of density limit are not changed at B_{t0}=1.26T (q_s=2.8) [23].

7. Summary

As the first stage of AMTEX program in the JFT-2M tokamak, the ferromagnetic FBs were inserted between VV and TFCs to reduce the toroidal field ripple. Local hot spots on the first wall due to RT and BD losses were detected during tangential co-NBI (36keV, ~500kW) by IRTV. Surface temperature on RT and BD loss regions reaches to ~120°C and ~190°C, and their hot spot locations agree well with an estimation from ripple well region before FB insertion. By FB1 (50mm thickness) insertion, a peak position of temperature increment due to RT loss shifted ~6cm outward in the major radius direction, and highest temperature increment $\Delta T_{s\text{-}max}$ was reduced to ~2/3 on both RT and BD loss regions. Furthermore, $\Delta T_{s\text{-}max}$ due to RT loss became almost negligible when FB thickness were increased to 67mm (FB2) and the shoulder part ripple δ_{16}^S was reduced to 0.07%. That corresponding to BD loss became also smallest. These results on RT loss consistent with the ripple reduction and the outward shift of ripple well boundary. In addition, we found out that the reductions of the fundamental mode ripple and the ripple banana diffusion coefficient at the shoulder part are most effective to reduce both RT and BD losses, respectively. The effect of second harmonic mode ripple may appear at equatorial plane to make the BD loss profile broaden together with reversal of fundamental mode ripple at low B_t with FB2. These were also confirmed at the experiment for the perpendicular beam injection.

The plasma production and control after FB insertion were done normally as before. Furthermore, the toroidal rotation velocity just inside of separatrix at H-mode with co-NBI became about twice larger than that without FB. This is favorable to avoid an occurrence of locked mode by the error fields. The regions of locked mode disruption and of density limit were not changed even though an error field was enhanced artificially to $B_{r\ (m/n=2/1)} / B_t \sim 1 \times 10^{-4}$ taking off 40% FBs.

In conclusion, the ferritic steel board inserted in JFT-2M is effective to reduce the toroidal magnetic field ripple and to reduce the fast ion losses, and does not have deteriorative effect on the plasma discharge.

Acknowledgment

The authors would like to acknowledge Dr. K. Tobita for valuable discussion and support regarding the ripple losses. We also thank Drs. H. Kishimoto, M. Azumi, A. Funahashi, A. Kitsunezaki and M.Shimizu for their support and encouragement.

References

[1] M. Tamura, H. Hayakawa, A. Yoshitake, A. Hishinuma and T. Kondo, J. Nucl. Mater. **155**, (1988) 620.
[2] K. Shiba, A. Hishinuma, A. Oyama and K. Masamura, JAERI-Tech 97-038 (1997).
[3] M. Abe, T. Nakayama, K. Asano and M. Otsuka, J. Plasma Fusion Res. **73**, (1997) 1283 (in Japanese).
[4] T. Nakayama, M. Abe, T. Tadokoro and M. Otsuka, J.Nucl. Mater. **271-272**, (1999) 491.
[5] L. R. Turner, S.T.Wang, H.C.Stevens, *Proc 3rd Topical Meeting on the Technology of Controlled Nuclear Fusion, Santa Fe*, (1978) 883.
[6] M. Ricci and N. Mitchell, Proc. *15th Symposium on Fusion Technology, Utrecht* (1988) 1565.
[7] G. V. Sheffield, PPPL-2876 (1993).
[8] M. Sato, Y. Miura, S. Takeji, H. Kimura and K.Shiba, J.Nucl. Mater. **258-263**, (1998) 1253.
[9] K.Tobita, H.Harano, T.Nishitani, T.Fujita, K.Tani, et al., Nucl. Fusion **37**, (1997) 1583.
[10] M.Sato, Y.Miura, H.Kimura, M.Yamamoto, et al., *Proc. of 20th SOFT (1998, Marselle)p.545*.
[11] M.Sato, Y.Miura, H.Kimura, H.Kawashima, S.Sengoku, et al., J. Plasma Fusion Res. **75**, 741(1999)
[12] M.Sato, H.Kawashima, Y.Miura, K.Tsuzuki, H.Kimura, et al., *Proc. of ISFNT (1999, Rome)*, to be published in Fusion Eng. Design.
[13] K.Tsuzuki, M.Sato, H.Kawashima, Y.Miura, et al., *Proc. of 9th ICFRM (1999, Colorado)*, to be published in J. Nucl. Matter.
[14] T.Nakayama, M.Yamamoto, M.Abe, T.Shibata, M.Ohtsuka, et al., *Proc. 18th SOFE (1999, Albuquerque)*.
[15] H.Kimura, H.Kawashima, K.Tsuzuki, M.Sato, Y.Miura, et al., JAERI-Conf 2000-004, (2000) 77.
[16] H.Kawashima, M.Sato, K.Tsuzuki, Y.Miura, H.Kimura et al., J. Plasma Fusion Research **76**, (2000) 585 (in Japanese).
[17] H.Kimura, M.Sato, H.Kawashima, N. Isei, K.Tsuzuki, et al., *Proc. of 21st SOFT (2000, Madrid), submitted to Fusion Eng. Design*.
[18] V. Ya. Goloborod'ko, et al., Physica Scripta T16, 46 (1987).
[19] H. Kawashima, K. Tsuzuki, T. Tani, M. Sato, H. Kimura and JFT-2M Group, *Proc of 13th Topical Conference on HTPD*, *EP2 (2000, Arizona)*.
[20] S.J. Zweben, R.V. Budny, D.S. Darrow, S.S. Medley, et al., Nucl.Fusion **40**, (2000) 91.
[21] K.Tobita, K.Tani, Y.Neyatani, A.A.E. van Blokland, S.Miura, et al., Phys. Rev. Lett. **23**, (1992)3060.
[22] R.J.LaHaye, et al., Phys. Fluids **B4**, (1992) 2098.
[23] N. Isei, M. Sato, K. Tsuzuki, H.Kawashima, Y.Miura, et al., to be presented at the *14th Topical Meeting on the Technology of Fusion Energy (Park City, USA)*.